Studies of the Conformation and Packing of Polysilanes

E. K. KariKari, A. J. Greso, and B. L. Farmer*

Department of Materials Science and Engineering, University of Virginia, Charlottesville, Virginia 22903-2442

R. D. Miller and J. F. Rabolt

Polymer Science and Technology, IBM Almaden Research Center, San Jose, California 95120-6099

Received November 9, 1992; Revised Manuscript Received April 5, 1993

ABSTRACT: A series of symmetric and asymmetric poly(di-*n*-alkylsilanes) have been investigated to assess their minimum-energy conformations, crystal packing, and, in the case of poly(di-*n*-tetradecylsilane) (PdnTDS), the conformation of the *n*-alkyl side chains. All of the polymers exhibit a thermochromic transition. X-ray diffraction measurements were made above and below the transition temperature to determine unit cell parameters for both the ordered and disordered phases. A TGTG′ silicon backbone conformation has been identified and found to occur routinely in symmetric poly(di-*n*-alkylsilanes) having side chain lengths between 9 and 14 carbon atoms. This unique conformation has previously been shown to be energetically feasible by molecular modeling calculations. Spectroscopic measurements on PdnTDS indicate that the side chains have predominantly an all-trans conformation. In all the polysilanes studied above their transition temperatures, it has been found that the backbone conformations become somewhat disordered, but the chains maintain a columnar arrangement on a hexagonal lattice. X-ray diffraction patterns from the disordered phases feature one strong and one or two weaker equatorial reflections. The *d*-spacing of the strongest reflection, which relates directly to the radius of the cylindrical molecular envelope, increases as the lengths of the *n*-alkyl side chains increase, apparently to accommodate the extra side chain length. The side chains themselves are disordered above the transition. Based on molecular models and the X-ray values of the cylindrical radii, the side chains are not extended but on average are shortened, presumably by the presence of one or more gauche bonds.

Introduction

The structures of poly(di-*n*-alkylsilanes) have been of great interest because of correlations between the UV–visible absorption, the chain conformation, the nature of the alkyl substituents, and the solid-state molecular packing.[1,2] The unusual and interesting electronic properties and the resulting optical absorption properties of these polymers make them potentially useful for a variety of technological applications.[2,3]

Poly(di-*n*-hexylsilane) (PdnHS) has a UV–visible absorption maximum at 370 nm at room temperature.[1] At 42 °C, the polymer undergoes a reversible structural transition whose manifestations can be observed by a variety of methods,[2-9] including IR and Raman spectroscopies and X-ray diffraction. Above this temperature, the absorption maximum shifts to 313 nm, and disordering of the conformation and molecular packing occurs.[9] Poly(di-*n*-pentylsilane) (PdnPS), in contrast, has an absorption at 313 nm[10] whose position does not change with temperature, even though PdnPS has a structural transition at 76 °C.[10] The considerably smaller enthalpy associated with the transition suggests a substantially different molecular mechanism than in PdnHS. Fiber diffraction patterns from oriented specimens of both polymers indicate that the orientation is retained above the transition temperature for prolonged periods and the original fiber patterns return when the samples are brought back to room temperature.[4,9,10]

X-ray diffraction measurements and conformational energy calculations have been used extensively to investigate the conformations of poly(di-*n*-alkylsilanes) having pentyl and hexyl substituents.[4-6,9-13] Using the layer line spacing from X-ray fiber patterns, it was found that PdnHS has a planar zigzag conformation at room temperature, characterized by a 4.0-Å chain repeat distance.[5,9,14] PdnPS has a chain repeat distance of 13.8 Å, corresponding to a 7/3 helical conformation,[10] with poly(di-*n*-butylsilane) adopting a similar structure.[15] Conformational energy calculations showed that both the planar zigzag and the helical conformations were low-energy conformations for both PdnHS and PdnPS, with the helical form being slightly lower in energy.[11,12] This suggested that the observed planar zigzag conformation of PdnHS was, in part, a result of *inter*molecular interactions[11,12] and the recently reported[14] structure of PdnHS is indicative of one which emphasizes inter- rather than intramolecular interactions. In essence, the planar zigzag form can pack somewhat more efficiently than the helical form, and thus it prevails at room temperature. It was further speculated[14] that the structural transition in PdnHS at 42 °C was associated with a breakdown of these intermolecular interactions, allowing the polymer to revert to a (lower conformational energy) helical form. This interpretation correlates well with experimental data from X-ray diffraction, vibrational spectroscopy, UV–visible absorption measurements, and NMR studies of the 42 °C transition.[1-11] Data on PdnPS, already helical at room temperature and not showing this transition, are consistent with this interpretation as well.[10,15] The smaller enthalpy associated with the 76 °C transition in PdnPS is rationalized by recognizing that, in this polymer, the transition represents a change in packing alone, whereas in PdnHS, the change is in both conformation and packing.

The position of the UV–visible absorption maximum can be correlated with the conformation (and structure) of the polymer. Molecular orbital calculations[16] of polysilane chains (having more computationally-manageable substituents than hexyl side chains) indicate a change in the delocalization in the σ bonding of the backbone as a function of torsion angle about the Si–Si bonds.[2,3,16] Clearly, the conformational transition from planar zigzag to helix is just such a change. Apparently, the absorption at 370 nm is associated with a trans (0°) torsion angle and

0024-9297/93/2226-3937$04.00/0

the delocalization it allows. Since the 313-nm absorption is observed in both helical and disordered conformations, it is likely that this absorption is not so much indicative of a particular torsion angle (such as 30° in the 7/3 helix), but rather that a 30° torsion results in the same delocalization (perhaps none) as a random conformation.

Poly(di-*n*-tetradecylsilane) (PdnTDS), having side chains of 14 methylene groups, has a thermochromic transition at 54 °C.[17] At room temperature, the polymer absorbs at 350 nm, a value coincidentally intermediate to those observed for PdnHS (370 nm) and PdnPS (313 nm). Above its transition, PdnTDS absorbs at 313 nm, as do the other poly(di-*n*-alkylsilanes) above their respective transition temperatures.[3,17]

Several asymmetric poly(*n*-alkyl-*n*-alkyl'silanes) have also been prepared and studied. Spectroscopic evidence[8] for poly(*n*-pentyl-*n*-hexylsilane) indicates that the defect associated with having *n*-pentyl and *n*-hexyl side chains mixed in the crystals interrupts the all-trans sequences of the silicon backbone. This is manifested by a lowering of the UV absorption maximum to 350 nm and the structural transition temperature to −5 °C.[8]

In this study, the unit cell dimensions and backbone conformations of a series of symmetrical and asymmetrical poly(di-*n*-alkylsilanes) have been determined using wide-angle X-ray diffraction (WAXD). In addition, the results of Raman and FT-Raman spectroscopic studies on PdnTDS are reported. This collective study of the structures of a series of symmetric poly(di-*n*-alkylsilanes) has provided further insight into the nature and role of side-chain interactions in determining the silicon chain conformation and solid-state packing of these σ-conjugated polymers. The structures adopted by some of the asymmetric polymers have also provided insight into the structural differences that arise between PdnPS and PdnHS.

Experimental Section

Diffraction. Films of each polymer sample were prepared by casting a viscous solution of the polymer in toluene onto a glass substrate. The solvent was evaporated, and the film was peeled from the substrate. Samples with low transition temperatures tended to be gummy and difficult to orient. Such orientation as could be induced was achieved by repeated rolling and/or stretching of the warm polymer. Differences in the degree and type of orientation achieved among the various samples would likely affect the relative intensities of reflections and would need to be considered in a full structural analysis. However, the layer line spacings (which yield the chain repeat distances) and the *d*-spacings of the observed reflections, which we consider here, should not be appreciably altered by the type or degree of orientation. The oriented samples were cooled for a period of time before diffraction patterns were obtained.

The diffraction patterns obtained at low, room, and elevated temperatures were recorded on flat photographic film in a Warhus camera. Low temperature was achieved by flowing methanol from a Neslab Endocal refrigerated circulating bath (ULT-80DD) through a copper block surrounding the sample holder. The camera was evacuated to reduce air scattering and ice buildup. Temperature control was obtained by cycling the control heater to the desired set point. A temperature stability of ±0.3 °C was attained. Elevated temperature was achieved using an electric heater controlled by an Omega Model 49 controller giving a temperature stability of ±0.5 °C. The samples were irradiated with nickel-filtered Cu Kα X-rays. Exposure times varied from 3 to 12 h. Powder diffractometer data were collected from some samples at a scan rate of 0.3° 2θ/min. Cu Kα X-rays and a germanium solid-state detector were used.

Density. Since only a small amount of material was available, density measurements were carried out using a hydrostatic weighing technique[18,19] based on the Archimedes principle. Using a microbalance, the sample was weighed in air and in an inert bouying fluid (2-methylene-1-pentanol) at various temperatures. The sample density is then easily determined when the density of the bouying fluid is known. In addition to being a nonsolvent for the sample, the selected buoyancy fluid offered the advantages of a high boiling point and a moderate surface tension.

Spectroscopy. Raman spectra were recorded with an Instruments SA HG-2S scanning double monochromator using the 4880-Å exciting line of a Spectra Physics 2020 argon ion laser operating at 300 mW of power. Detection of the scattered photons by an RCA 31034A-02 photomultiplier facilitated the recording of Raman spectra such that only five scans needed to be coadded in order to obtain a high S/N ratio spectrum. The powdered sample was contained in a 1.2-mm-diameter capillary which could then be held in a thermostated Harney–Miller cell for variable-temperature measurements.

The FT-Raman instrument was a prototype design constructed in 1986 using a Bomem DA 3.02 Michelson interferometer and Spectron SL50 Nd/YAG laser operating at 1.064 μm and a right-angle collection system using transmissive optics. The primary purpose for using FT-Raman spectroscopy to investigate PdnTDS was to remove all traces of resonance interactions in the spectrum. The excitation wavelength (1.064 μm) used in this experiment is far removed from the UV–visible absorption of PdnTDS at 350 nm, and hence no resonance enhancement of selected band intensities occurs.

Results

Symmetric Poly(di-*n*-alkylsilanes): Pentyl, Heptyl, and Octyl. The *d*-spacings observed for a series of poly(di-*n*-alkylsilanes) at temperatures below their respective transitions are listed in Table I. The derived unit cell dimensions are summarized in Table II. For comparison, cell dimensions reported by others are also included in the table. The reflection data taken above the transition temperatures are shown in Table III.

The diffraction pattern (Figure 1) for PdnPS showed sharp reflections to about 4 Å, compared to about 1.2 Å for PdnHS. An intense near-meridional reflection on the third layer line at a *d*-spacing of 4.49 Å was indexed as (013). A diffraction pattern obtained by rotating the sample normal to the orientation axis revealed an (007) reflection, indicating (as reported earlier[10]) that the polymer adopts a 7/3 helical backbone conformation. The *d*-spacings (Table I) can be indexed by a monoclinic unit cell with dimensions a = 13.8 Å, b = 23.8 Å, c = 13.8 Å, and γ = 120°. The diffraction pattern at elevated temperature (above 76 °C) changes in a fashion analogous to that of PdnHS. At 110 °C, most of the sharp reflections have smeared out into an amorphous halo, leaving only zero layer reflections at 12.1, 6.99, and 6.05 Å. The ratio of the observed *d*-spacings is $1:3^{1/2}:2$, suggesting a columnar packing of the polymer molecules on a hexagonal lattice.[20] These can be indexed as the 100, 110, and 200 reflections of a metrically hexagonal unit cell having dimensions a = b = 14.0 Å.

The diffraction pattern shown in Figure 2 for an oriented sample of poly(di-*n*-heptylsilane) at 0 °C showed 15 reflections over an angular range between 6 and 32° 2θ. Comparison of the diffraction patterns clearly shows that the low-temperature structure in poly(di-*n*-heptylsilane) is far less ordered than that of PdnHS. The moderate orientation results in generally long arcs which can be seen to concentrate on layer lines consistent with an all-trans conformation. The strong near-meridional reflection at a *d*-spacing of 3.84 Å is interpreted to be a pair of smeared {111} reflections. This is in keeping with the observed result of misorientation in PdnHS, where such lines are seen to smear together on the meridian. The pattern for poly(di-*n*-heptylsilane) can be indexed by an orthorhombic unit cell having dimensions a = 14.7 Å, b = 27.4 Å, and

Table I. WAXD Data for Poly(di-*n*-alkylsilanes) below Their Transition Temperatures

hkl	d_{obs}	d_{calc}	*hkl*	d_{obs}	d_{calc}
(i) Poly(di-*n*-pentylsilane) at Room Temperature					
100	11.83	11.92	013	4.49	4.49
110	8.53	8.62	2,–4,2	4.30	4.30
2,–1,0	6.67	6.68	050	4.13	4.13
200	5.96	5.96	132	4.04	4.04
130	4.98	4.97	1,–3,3	3.98	3.98
131	4.65	4.68	060	3.44	3.44
(ii) Poly(di-*n*-heptylsilane) at 0 °C					
100	14.70	14.68	011	3.98	3.98
020	13.71	13.69	111	3.84	3.84
130	7.82	7.75	221	3.42	3.41
200	7.33	7.34	051	3.24	3.25
220	6.45	6.47	301	3.09	3.09
150	5.13	5.13	061	3.03	3.03
300	4.89	4.90	261	2.83	2.83
(iii) Poly(di-*n*-octylsilane) at Room Temperature (Trans)					
100	16.43	16.43	250	4.82	4.91
110	14.37	14.37	070	4.25	4.23
130	8.41	8.47	101	3.91	3.89
210	7.76	7.92	360	3.65	3.67
220	7.17	7.19	370	3.35	3.35
320	5.10	5.14	520	3.20	3.21
(iv) Poly(di-*n*-octylsilane) at Room Temperature (TGTG′)					
110	14.73	14.75	150	4.24	4.25
200	10.02	10.04	241	4.07	4.08
210	9.10	9.12	002	3.94	3.92
130	6.83	6.81	520	3.77	3.77
400	5.02	5.02	260	3.41	3.41
321	4.60	4.61			
(v) Poly(di-*n*-nonylsilane) at Room Temperature					
110	15.66	15.86	161	3.63	3.63
020	12.58	12.56	222	3.51	3.51
210	9.56	9.45	071	3.26	3.26
130	7.77	7.75	630	3.16	3.16
400	5.13	5.12	412	3.08	3.08
241	4.42	4.42	123	2.53	2.53
(vi) Poly(di-*n*-decylsilane) at Room Temperature					
110	16.29	16.26	401	4.39	4.41
210	9.84	9.85	002	3.89	3.89
220	8.15	8.13	501	3.77	3.76
330	5.41	5.42			
(vii) Poly(di-*n*-undecylsilane) at Room Temperature					
110	16.30	16.37	140	6.01	6.01
210	9.91	9.93	401	4.43	4.44
030	8.40	8.34	002	3.90	3.92
130	7.75	7.76	501	3.79	3.78
(viii) Poly(di-*n*-dodecylsilane) at Room Temperature					
110	16.72	16.74	411	4.44	4.44
210	10.28	10.11	002	3.92	3.92
220	8.37	8.37	262	2.80	2.80
140	6.19	6.19			
(ix) Poly(di-*n*-tetradecylsilane) at Room Temperature					
110	17.32	17.39	310	6.93	6.98
200	10.59	10.78	401	4.46	4.45
210	9.87	9.83	351	3.95	3.95
220	8.68	8.70	002	3.95	3.95

c = 4.0 Å. Assuming two molecules per unit cell, the X-ray density calculated from these cell dimensions is 0.93 g/cm^3, a value comparable to the measured densities of other polysilanes. The chain repeat distance of 4.0 Å is consistent with an all-trans backbone conformation. Similar to PdnHS, most of the sharp reflections disappear when the sample is heated to 65 °C, with only three sharp zero layer reflections remaining at 14.1, 8.12, and 7.03 Å. These were accompanied by an amorphous halo centered at about 3.7 Å. The high-temperature spacings are consistent with a columnar hexagonal packing with $a = b$ = 16.2 Å.

Table II. Unit Cell Dimensions and Conformations of Di-*n*-alkyl and *n*-Alkyl-*n*-alkyl′ Polysilanes

polymer	a, Å	b, Å	c, Å	γ, deg	backbone	ref
dimethyl	12.2	8.0	3.88	90	trans	22
diethyl	11.1	12.1	3.99	90	trans	23
di-*n*-propyl	9.8	9.8	3.99	90	trans	23
di-*n*-butyl	12.8	22.2	13.9	120	7/3 helix	7
di-*n*-pentyl	13.8	23.8	13.8	120	7/3 helix	
di-*n*-hexyl	13.8	21.9	4.1	90	trans	5, 9
di-*n*-heptyl	14.7	27.4	4.0	90	trans	
di-*n*-octyl	16.4	26.4	4.0	90	trans	
di-*n*-octyl	20.1	21.7	7.8	90	TGTG′	
di-*n*-nonyl	20.5	25.1	7.8	90	TGTG′	
di-*n*-decyl	21.4	24.9	7.8	90	TGTG′	
di-*n*-undecyl	21.6	25.0	7.8	90	TGTG′	
di-*n*-dodecyl	22.0	25.8	7.8	90	TGTG′	
di-*n*-tetradecyl	21.5	29.5	7.9	90	TGTG′	
propylmethyl	9.6	13.1	4.0	90	trans	
pentylhexyl	14.7	25.4	4.0	120	trans	
hexylheptyl	14.1	25.0	4.0	90	trans	

Table III. WAXD Data above the Structural Transition Temperatures

polymer	d_{100}	d_{110}	d_{200}	cell dimens
di-*n*-butyl	11.50			$a = b$ = 13.3
di-*n*-pentyl	12.12	6.99	6.05	$a = b$ = 14.0
di-*n*-hexyl	13.50	7.75		$a = b$ = 15.5
di-*n*-heptyl	14.10	8.12	7.03	$a = b$ = 16.2
di-*n*-octyl	15.46	8.95	7.85	$a = b$ = 17.9
di-*n*-nonyl	15.94	9.17	7.98	$a = b$ = 18.4
di-*n*-decyl	16.52	9.54	8.25	$a = b$ = 19.1
di-*n*-undecyl	17.75	10.23		$a = b$ = 20.5
di-*n*-dodecyl	18.06			$a = b$ = 20.8
pentylhexyl	12.90	7.46	6.46	$a = b$ = 14.9
hexylheptyl	13.72	7.93		$a = b$ = 15.3

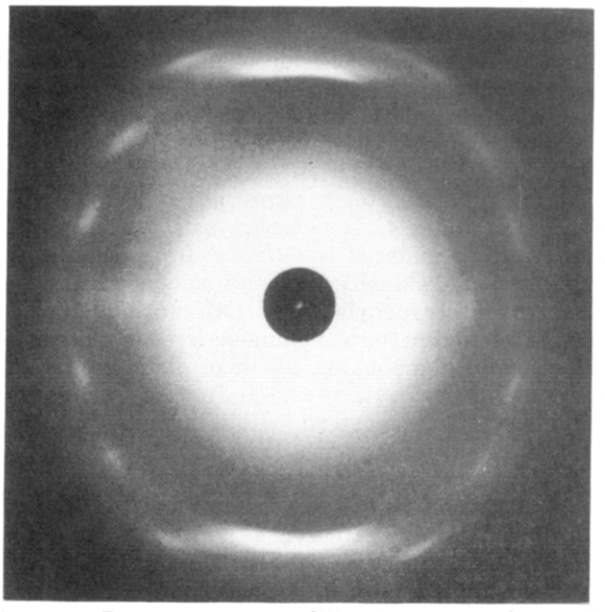

Figure 1. Room-temperature diffraction pattern from poly(di-*n*-pentylsilane).

Two distinctly different diffraction patterns have been obtained from poly(di-*n*-octylsilane). The pattern shown in Figure 3a is characteristic of an all-trans conformation, while the other (Figure 3b) is like that obtained from polymers having longer side chains. The data and unit cells from both are presented in the tables. The two samples were separated from a reaction product which had a bimodal molecular weight distribution. The higher molecular weight material (M_w = 10^6; M_w/M_n = 2.0) was isolated as a slightly sticky white solid, while the lower molecular weight material (M_w = 32 000; M_w/M_n = 2.3) was more powdery. The higher molecular weight material

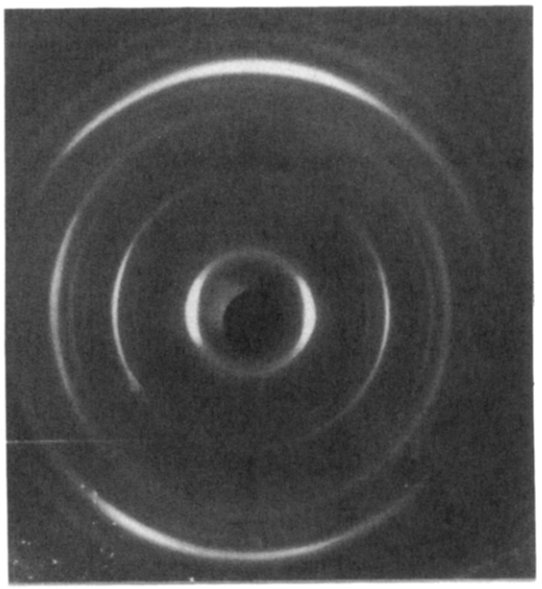

Figure 2. Diffraction pattern from poly(di-*n*-heptylsilane) obtained at 0 °C.

adopts the all-trans conformation. It seems unlikely that molecular weight differences alone would give rise to different crystalline structures, but the presence of residual solvent or other impurity in the higher molecular weight polymer (indicated by its stickiness) could be a possible explanation for the observed structural differences.

The WAXD diffraction patterns obtained at low temperature from samples of poly(di-*n*-nonyl-, di-*n*-decyl-, di-*n*-undecyl-, di-*n*-dodecyl-, and di-*n*-tetradecylsilanes) show that the polymer backbone deviates from an all-trans conformation when side chains of nine or more methylene units are appended to the silicon backbone. The best orientation was achieved in PdnTDS. Its conformation is consistent with and provides a basis for interpreting the diffraction patterns from this set of polymers. The room-temperature pattern from PdnTDS is shown in Figure 4. It clearly reveals that the conformation of the material is different from the all-trans conformation of PdnHS or the 7/3 helix of PdnPS.

Poly(di-*n*-tetradecylsilane). Diffraction. The PdnTDS diffraction pattern is characterized by quite sharp reflections on the equator, a pair of distinctly broader reflections on the first layer line, and a strong second layer meridional reflection at 3.95 Å. The layer line spacing is 7.9 Å. Fiber patterns obtained from an intentionally tilted fiber showed a meridional reflection on the fourth layer line also. The repeat distance is intermediate to those of PdnHS and PdnPS and thus suggests a conformation "intermediate" to those of PdnHS and PdnPS. However, numerically intermediate torsion angles (between 0° for trans and 30° for the 7/3 helix) in fact give helices having *longer* repeat distances rather than shorter. On the other hand, a TGTG′ bond rotation sequence gives a repeat distance in the range of 7.6 Å, with the minimum-energy geometry having backbone bond lengths and angles of 2.42 Å and 121°, respectively, and a "gauche" rotation value of 126° (trans = 0°). Molecular mechanics calculations show this conformation (for PdnHS) to be comparable in energy to other low-energy conformations observed for the polysilanes.[12] In fact, the TGTG′ conformation is comparable in energy to the all-trans conformation and only somewhat higher than the helical conformation.[12]

For the TGTG′ backbone conformation and fully extended side chains, the cross section of the PdnTDS

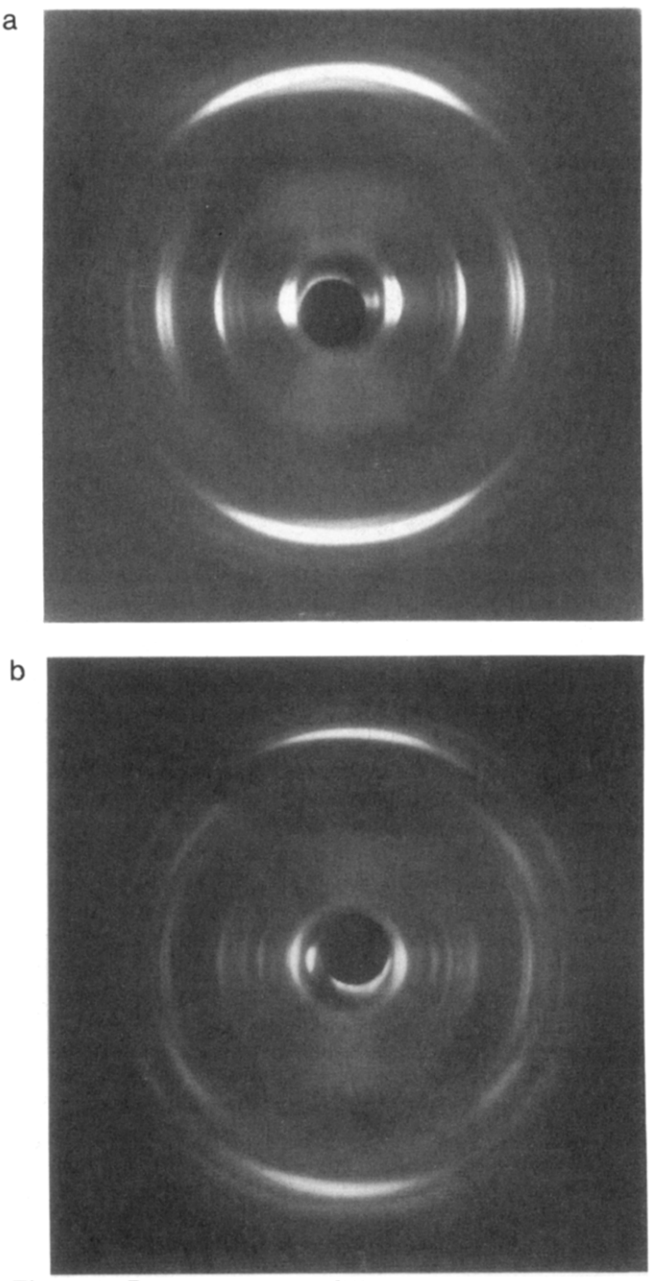

Figure 3. Room-temperature diffraction patterns from poly(di-*n*-octylsilane), showing all-trans (a) and TGTG′ (b) conformations.

molecule would extend almost 38 Å. Although it would be somewhat smaller if the side chains were in fact not all-trans, it is not surprising that the unit cell would be large. Using *d*-spacings from powder diffractometer data and from film readings, it is found that an orthorhombic unit cell having dimensions a = 21.5 Å, b = 29.5 Å, and c = 7.9 Å gives *d*-spacings in reasonable agreement with the observed values. The crystalline density calculated from these cell dimensions is 1.01 g/cm^3. The diffraction pattern obtained at 76 °C suggests that the structural changes at the transition are similar in nature to those observed in the other polysilanes,[3,20] namely, that molecules assume a somewhat disordered backbone conformation and, in their resulting cylindrical shape, arrange themselves in a columnar hexagonal packing mode.

The measured density of a sample of PdnTDS as a function of temperature is shown in Figure 5. Condensation of the bouyancy fluid on the sample and weighing pan precluded measurements up to and through the transition temperature. The density at room temperature

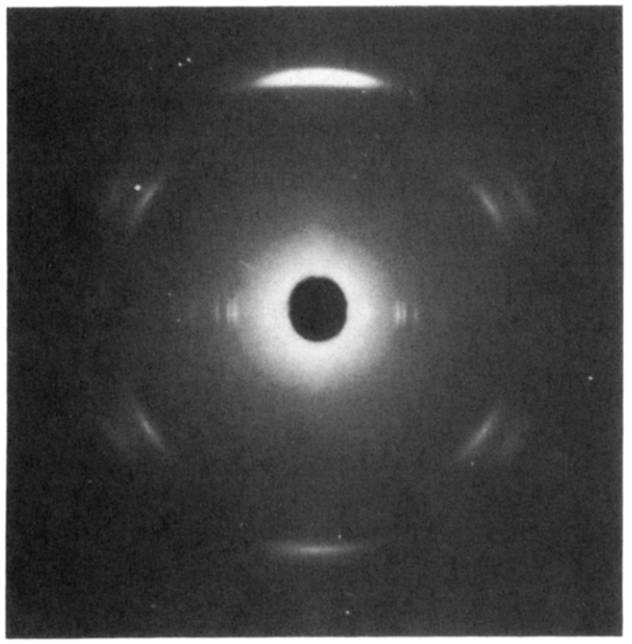

Figure 4. Room-temperature diffraction pattern from poly(di-*n*-tetradecylsilane).

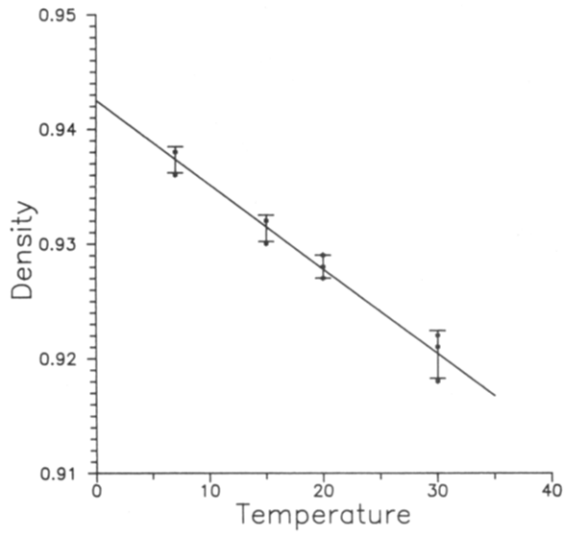

Figure 5. Density versus temperature for poly(di-*n*-tetradecylsilane).

is about 0.925 g/cm^3, and the volumetric thermal expansion coefficient is 8.0×10^{-4} °C^{-1}. These compare to values of 0.925 g/cm^3 and 8.4×10^{-4} °C^{-1}, respectively, for PdnHS at room temperature.

Spectroscopy. Since Raman spectroscopy has proven to be a valuable tool for investigating local conformational order in previous studies[8-10] of planar zigzag and 7/3 helical poly(di-*n*-alkylsilanes), a study of the conformational structure of PdnTDS was undertaken. As shown in Figure 6, the room-temperature Raman spectrum of PdnTDS is significantly different from that of planar zigzag PdnHS. The most obvious difference is the absence of the intense, resonantly-enhanced band at 689 cm^{-1} attributed to the symmetric Si–C stretch and the 375-cm^{-1} Si–Si symmetric stretching vibration. Interestingly, the remaining portion of the spectrum of PdnTDS below 800 cm^{-1} contains bands which are characteristic of both helical (490 and 675 cm^{-1}) and planar zigzag (470 cm^{-1}) conformations. In retrospect, this is not too surprising since the TGTG′ conformation of PdnTDS contains both trans and gauche bonds. One band which appears to be unique to PdnTDS is the intense

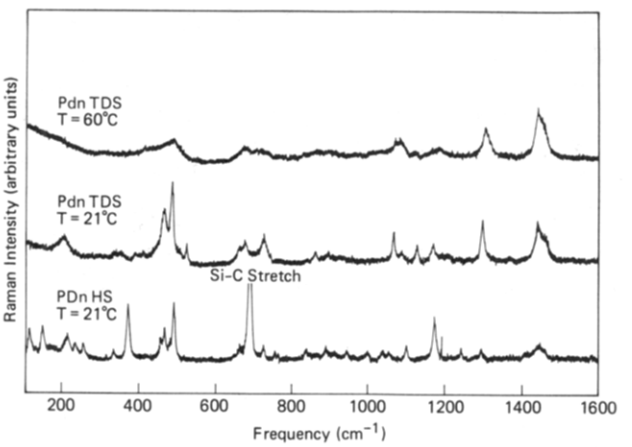

Figure 6. Raman spectra of poly(di-*n*-tetradecylsilane) compared to that of poly(di-*n*-hexylsilane) (exciting line, 4880 Å).

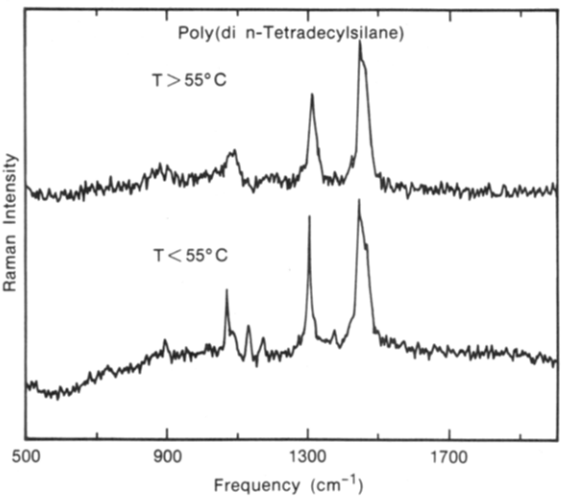

Figure 7. FT-Raman spectra of poly(di-*n*-tetradecylsilane) (exciting line, 1.064 μm).

peak found at 485 cm^{-1}, most likely assignable to the symmetric Si–Si stretching vibration of the TGTG′ backbone. Its position falls coincidentally between the identical vibrations for the trans (470 cm^{-1}) and helical (495 cm^{-1}) conformations.

There are also significant differences in the spectra of PdnTDS and PdnHS above 1000 cm^{-1}, where primarily vibrations due to the *n*-alkyl side chains can be found. Since the *n*-alkyl side chains of PdnTDS are considerably longer than those of PdnHS, the intensities of these bands in the PdnTDS spectrum are considerably higher. The FT-Raman spectrum of this region, obtained using near-IR excitation, is shown in Figure 7. Upon close inspection, it is clear that bands are present at 1060 and 1130 cm^{-1} which are characteristic of trans planar *n*-alkyl chains. This suggests that the *n*-tetradecyl side chains adopt an all-trans conformation. The presence of a shoulder at 1080 cm^{-1} may be indicative of gauche bonds which may occur at the Si–C bond or the C–C adjacent to it. The presence of gauche bonds near the silicon backbone, which are due to steric effects in this crowded region, is consistent with conformational energy calculations.[12,14]

Other information about packing of the *n*-tetradecyl side chains can be obtained by considering the intensity pattern of the CH_2 bending region at 1450 cm^{-1}. Both the number of bands present and their relative intensities have been shown[8] to be indicative of the packing of *n*-alkyl chains in a unit cell. The rather simple pattern shown in Figure 7 is characteristic of a hexagonal subcell, indicating that the side chains have only weak intermolecular

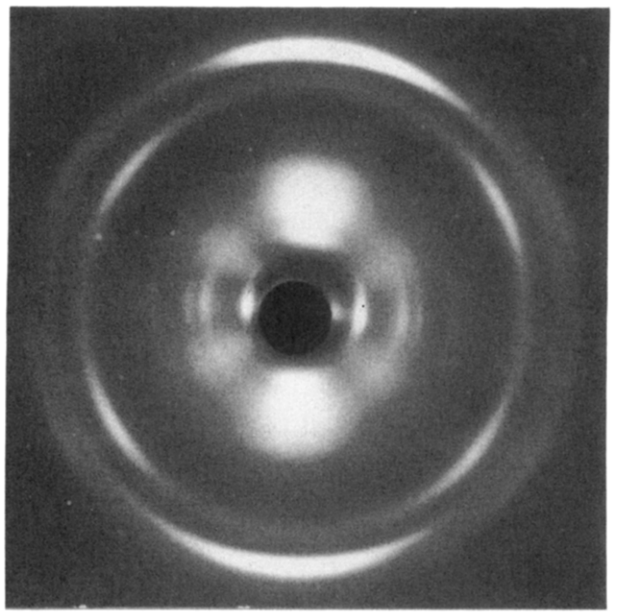

Figure 8. Room-temperature diffraction pattern from poly(di-*n*-dodecylsilane).

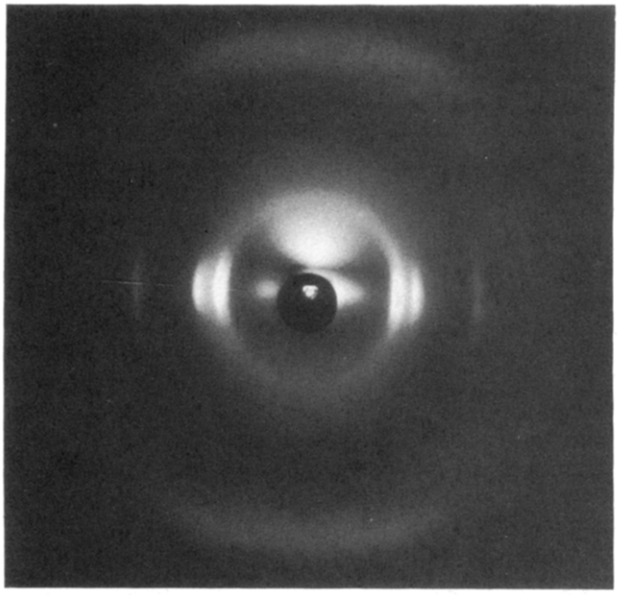

Figure 9. Room-temperature diffraction pattern from poly(methyl-*n*-propylsilane).

interactions. This is further supported by the elevated-temperature spectrum of PdnTDS shown in the upper portion of Figure 7. When PdnTDS is heated above its transition temperature, where intermolecular interactions are minimal, the 1450-cm^{-1} band shape changes only slightly, indicating that the room-temperature spectrum represents *n*-tetradecyl side chains which do not interact significantly. On the other hand, in the 1000-1150-cm^{-1} region, the upper spectrum of Figure 7 does differ considerably from that obtained at room temperature. The sharp bands at 1060 and 1130 cm^{-1}, characteristic respectively of the asymmetric and symmetric C–C stretching vibrations of a planar zigzag structure, have been replaced by a broad weak band at 1080 cm^{-1} attributable to the presence of gauche bonds. Hence, these results indicate that the *n*-tetradecyl side chains are considerably disordered above the transition temperature. Taken together with the general smearing of bands in the Si–Si stretching region (400-500 cm^{-1}) and the Si–C stretching region (650–750 cm^{-1}) shown in the upper spectrum of Figure 6, suggesting that the backbone also becomes disordered above the transition temperature, it becomes clear that PdnTDS undergoes an order–disorder transition at 55 °C. Similar conclusions were obtained previously for PdnHS and PdnPS.[21]

Symmetric Poly(di-*n*-alkylsilanes): Nonyl, Decyl, Undecyl, and Dodecyl. The diffraction pattern for poly(di-*n*-nonylsilane) at room temperature is similar to that for poly(di-*n*-dodecylsilane) shown in Figure 8. Fifteen reflections were observed between 5 and 40° 2θ. The room-temperature *d*-spacings can be indexed by an orthorhombic unit cell with dimensions a = 20.5 Å, b = 25.1 Å, and c = 7.8 Å. A striking feature of the diffraction pattern is again an intense meridional reflection on the 2nd layer line at a *d*-spacing of 3.90 Å. This reflection was identified as (002), giving a chain repeat distance consistent with a TGTG′ backbone conformation. Above the transition temperature, the diffraction pattern changes in a manner similar to the changes observed for the other polysilanes. The high-temperature pattern is dominated by an intense zero layer reflection at 15.9 Å accompanied by two relatively weak ones at 9.17 and 7.98 Å. These are consistent with 100, 110, and 200 reflections of a hexagonal unit cell with $a = b$ = 18.4 Å. Nonequatorial reflections blurred into an amorphous halo centered at about 4 Å.

The WAXD pictures of poly(di-*n*-decyl- and di-*n*-undecylsilanes) are similar to those for poly(di-*n*-dodecylsilane) and PdnTDS with an intense reflection at 3.9 Å on the meridian of the X-ray patterns, indicative of the TGTG′ conformation. The unit cells consistent with the observed *d*-spacings are given in Table II. A diffuse reflection appears on the meridian in each of these patterns at a *d*-spacing of ~13.6 Å. The possibility of the presence of a second partially ordered phase was considered, perhaps T_3GT_3G', which would have a repeat distance on the order of 13 Å. The reflection does not appear in the diffraction patterns obtained above the transition temperature, thus eliminating the possibility of its origin being the disordered helical conformation[3] which polysilanes are presumed to adopt above their transition temperatures. The diffuse reflection also does not appear in patterns made using a graphite monochromator and thus appears to be a white radiation streak associated with the (002) reflection or with extraneous wavelengths from the X-ray tube used. The energetics of a T_3GT_3G' were investigated, nonetheless.

The elevated temperature diffraction patterns for poly(di-*n*-decyl-, di-*n*-undecyl-, and di-*n*-dodecylsilanes) are similar to those from other polysilanes. Each diffraction pattern was dominated by an intense equatorial reflection accompanied by a diffuse halo at ~4.0 Å. The remaining reflections were consistent with a metrically hexagonal packing mode.

Asymmetric Poly(*n*-alkyl-*n*-alkyl′silanes). Shown in Figures 9–12 are the WAXD patterns of the asymmetric polymers. All reveal a low degree of crystallinity and ordering compared to the symmetric poly(di-*n*-alkylsilanes). Their asymmetry and atacticity preclude perfect ordering because of the unavoidable defects associated with having different side-chain lengths mixed in the crystals. The *d*-spacings observed for these polymers are given in Table IV, and the unit cell dimensions are included in Table II.

The WAXD pattern for poly(methyl-*n*-propylsilane) obtained at room temperature (Figure 9) showed only four reflections in the pattern from a modestly oriented sample. Two strong and one weaker reflection (at 9.62 Å) appeared on the equator. A relatively diffuse reflection appeared on (presumably) the first layer line at a *d*-spacing of ~3.84 Å. Cooling the sample to −40 °C did not improve the

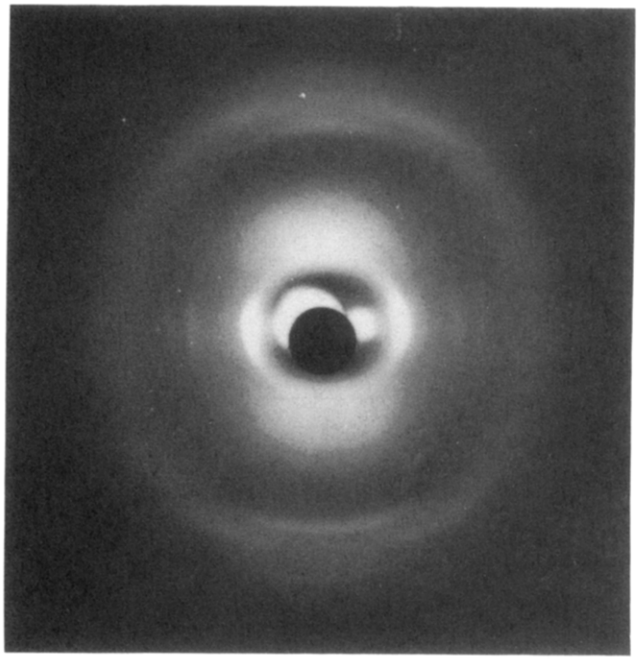

Figure 10. Diffraction pattern from poly(*n*-butyl-*n*-hexylsilane) at −30 °C.

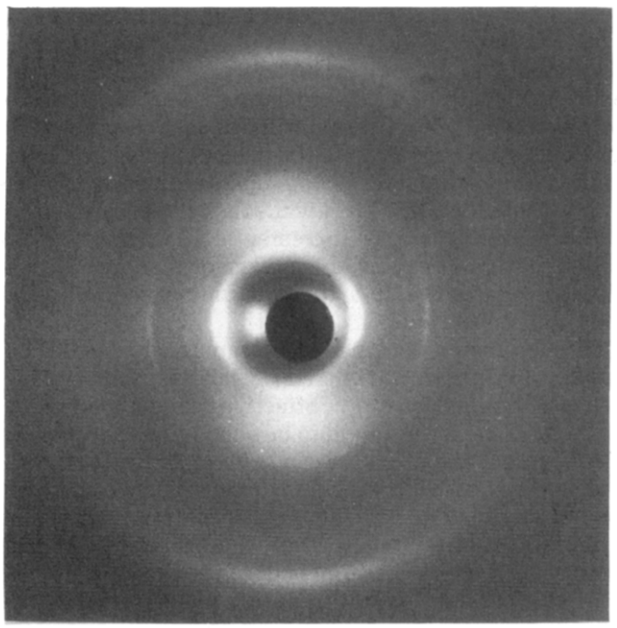

Figure 11. Diffraction pattern from poly(*n*-pentyl-*n*-hexylsilane) at −40 °C.

pattern. The diffraction pattern is characteristic of the polysilanes having an all-trans conformation. It is not surprising that the polymer adopts such a conformation because the symmetric polymer of either substituent adopts an all-trans conformation.[22] The polymer behaves differently from the other asymmetric ones studied here in that, at room temperature, it exists in the ordered form. The others are disordered at room temperature.

Somewhat surprisingly, the diffraction pattern (Figure 10) for an oriented sample of poly(*n*-butyl-*n*-hexylsilane) at −30 °C was similar to that obtained[23] for poly(di-*n*-butylsilane) (PdnBS) which adopts a 7/3 helical backbone conformation. The diffraction pattern reveals an intense near-meridional reflection at ~4.7 Å (as compared to 4.6 Å for PdnBS). Unlike the sharp reflections for PdnBS, however, the pattern for poly(*n*-butyl-*n*-hexylsilane) showed disordering, with no reflections appearing on the first and second layers. Three zero layer and two upper

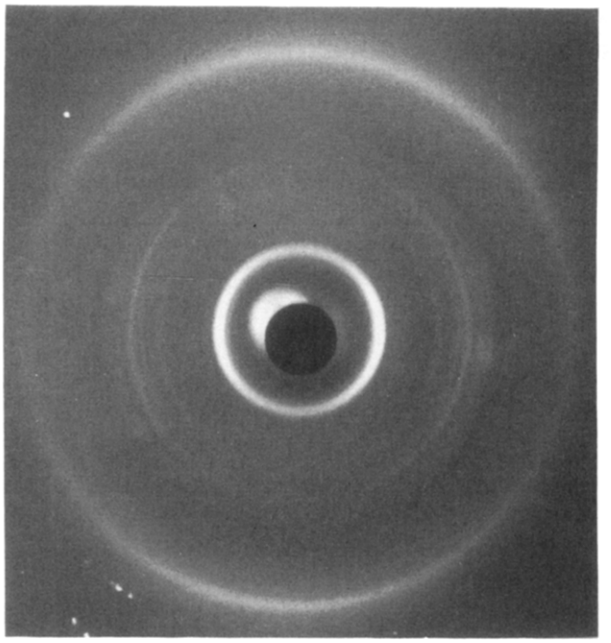

Figure 12. Diffraction pattern from poly(*n*-hexyl-*n*-heptylsilane) at −40 °C.

Table IV. WAXD Data for Poly(*n*-alkyl-*n*-alkyl′silanes)

hkl	d_{obs}	d_{calc}	*hkl*	d_{obs}	d_{calc}
(i) Poly(*n*-propyl-*n*-methylsilane) at Room Temperature					
100	9.62	9.65	120	5.39	5.39
110	7.71	7.71	011	3.84	3.84
(ii) Poly(*n*-pentyl-*n*-hexylsilane) at −40 °C					
100	12.66	12.56	030	5.87	5.87
120	7.16	7.20	130	5.31	5.31
200	6.29	6.29	101	3.82	3.82
(iii) Poly(*n*-hexyl-*n*-heptylsilane) at −40 °C					
100	13.99	14.05	310	4.60	4.60
130	7.18	7.17	320	4.38	4.39
210	6.76	6.76	011	4.11	4.11
040	6.25	6.26	121	3.81	3.81
140	5.70	5.70			

layer reflections could be identified. At room temperature the material is disordered with only an intense zero layer reflection appearing in the diffraction pattern.

The diffraction pattern for poly(*n*-pentyl-*n*-hexylsilane) shown in Figure 11 lacks the sharpness observed for PdnHS. Even at −40 °C, only five zero layer reflections were observed for this asymmetric polymer. A sharp reflection on the first layer line, indexed as a (101) reflection, could be identified in the diffraction pattern for the modestly oriented sample. The polymer chain repeat distance of 4.0 Å is indicative of an all-trans backbone conformation.

The poly(*n*-hexyl-*n*-heptylsilane) showed a similar diffraction pattern (Figure 12) at −40 °C. Seven zero layer reflections were observed. A strong reflection on the first layer line at 3.81 Å was indexed as (121). The chain repeat distance is again consistent with an all-trans silicon backbone conformation.

Except for poly(methyl-*n*-propylsilane), which is ordered at room temperature, the asymmetric polymers showed room-temperature diffraction patterns similar to those of the symmetrical polymers above their transition temperatures. Three zero layer reflections were observed in the room-temperature diffraction pattern of poly(*n*-pentyl-*n*-hexylsilane). These were indexed as (100), (110), and (200) reflections of a hexagonal unit cell with $a = b = 14.9$ Å. In the case of poly(*n*-hexyl-*n*-heptylsilane), only two

Table V. Relative Energies for TTTGTTTG′ Conformation

Si–C torsion	energy (kcal/mol)	Si–C torsion	energy (kcal/mol)
240	26.6	215	23.9
230	23.6	35	32.6
220	23.8	30,50	31.4

Table VI. Relative Energies Calculated for Poly(di-*n*-hexylsilane)[10]

conformn	side-chain torsion	energy (kcal/mol)
trans	35	23.4
trans	200	18.1
30 (7/3 helix)	15	18.6
30 (7/3 helix)	245	12.8
TGTG′	30,50	22.4
gauche	210	19.1

reflections were observed at 13.7 and 7.93 Å. The *d*-spacings are consistent with a hexagonal unit cell with dimensions $a = b = 15.3$ Å.

Conformational Energy Calculations. The presence of the diffuse meridional diffraction from the polysilanes having long side chains suggested the possibility of a low-energy conformation having a repeat distance of about 13 Å. Using a Si–Si bond length of 2.35 Å and backbone valence angle of 112°, the repeat distance for a T_3GT_3G' conformation is 13.6 Å, consistent with the value measured on the X-ray film for di-*n*-nonyl, di-*n*-decyl, di-*n*-undecyl, di-*n*-dodecyl, and di-*n*-tetradecyl polysilanes. Molecular mechanics calculations were therefore used to explore structures having this conformation. In general, intermolecular interactions serve to influence a polymer's selection of a conformation from among various low-energy possibilities. High-energy conformations typically do not benefit sufficiently from intermolecular interactions to make them energetically feasible. Thus, calculations on an isolated PdnHS molecule in a T_3GT_3G' conformation were carried out using SYBYL molecular modeling software, version 5.2,[24] which utilizes a molecular mechanics optimization method to determine low-energy structures. So that the energies could be compared with previous results,[12] full-relaxation energy minimization was carried out on a model consisting of eight silicon atoms and their associated hexyl side chains. A full description of the force field and parameterization employed in these calculations has been published previously.[12] Results of the conformational calculations on T_3GT_3G' are presented in Table V. Energy values are given on the basis of two silicon atoms with associated side chains. For comparison, Table VI shows the results from previous work[12] on PdnHS. Though ultimately the diffuse X-ray reflection was attributed to other sources, the energy calculations show that a T_3GT_3G' backbone conformation is energetically possible for polymers of this type. The model used in this calculation, however, is representative of only one repeat unit of the polymer chain. A longer chain segment would be needed to eliminate the possible influence of end effects on the energies.

Clearly, since all calculations were made on PdnHS, no conclusions can be drawn from these calculations concerning the effects of side-chain length. Pentyl and hexyl side chains do not change the relative energies of the various silicon backbone conformations. However, longer side chains may well make some conformations more favorable than others, as perhaps by their ability to pack themselves in alkane-type structures. Calculations investigating this possibility along with the influence of intermolecular packing energies are currently underway.

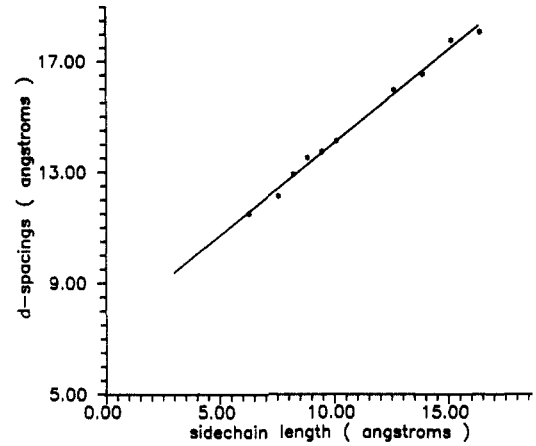

Figure 13. Observed *d*-spacing versus side-chain length of polysilanes above their respective structural transition temperatures.

Discussion

Figure 13 shows a plot of the *d*-spacings of the intense reflections from the high-temperature diffraction patterns of all the poly(*n*-alkylsilanes) studied thus far. The straightness of the least-squares straight line suggests that all the polymers have a similar structure, described[20] as columnar hexagonal packing of cylindrical molecules. The slope of the line (0.67 Å/Å) indicates that, for each additional 1.27 Å that a methylene unit would add to the extended length of a side chain, the *d*-spacing increases by only 0.85 Å. For columnar hexagonal packing of the molecules, this increase in the *d*-spacing implies an increase in the cylinder diameter of 1.0 Å upon adding a methylene unit to the side chain. Thus, while the cylindrical envelope of the molecule increases incrementally as methylenes are added to the side chains, the increment is about 25% less (1.0 Å compared to 1.27 Å) than the amount the methylene unit adds to the side-chain length.

Measurements were made on computational molecular models of PdnHS in disordered 7/3 helical and all-gauche[20] helical conformations. The effective cylinder diameter of a static 7/3 helix was found to be about 19 Å (allowing for a 2-Å contact distance between helices). That for the all-gauche helix, also allowing for contact distances between helices, was found to be about 22 Å. Results from molecular dynamics studies[25] show that the cylinder diameter decreases by about 4 Å as a result of the tendency for one bond in each side chain to adopt a gauche conformation. This would leave the 7/3 helix with a diameter of about 15 Å, consistent with the observed *d*-spacing of 13.5 Å (which corresponds to a diameter of 15.5 Å). The cylinder diameter of the all-gauche helix would decrease to about 18 Å, giving a *d*-spacing of about 15.7 Å, a value significantly greater than the observed value. However, the all-gauche helix, by interdigitating side chains, might also be consistent with this dimension, as pointed out previously.[20]

One feature of the PdnTDS diffraction pattern is particularly intriguing and warrants further comment. All the diffraction spots (both zero and upper layer) in the pattern obtained from PdnHS are similar in their sharpness, and as previously noted[9] the sharpness of the pattern is somewhat unusual for diffraction from a polymer. The pattern for PdnPS is more typical of polymer diffraction patterns, but again the spots are all similar in character—in this case, their breadth. The pattern from PdnTDS is strikingly different. The zero layer spots are remarkably sharp, whereas the upper layer spots are quite broad. At a minimum, this indicates that the lateral packing of the molecular envelopes of the polymer chains is much better

defined than is the detailed packing of the side chains. It could be speculated that the upper layer lines have distinct diffraction maxima because of the packing of the side chains attached to individual silicon backbones but that there is little or no registration between adjacent polymer molecules. Can the diffraction pattern then be analyzed on the basis of two lattices—one corresponding to a more or less hexagonal packing of the polymer envelopes and the other a paraffin-like lattice whose chain axis dimension is oriented transverse to the silicon chain axis? Side-chain crystallization into crystallites on the order of 30–40 Å, superimposed on the larger scale arrangement of the silicon backbones, may be a useful model for describing this structure. The diffraction maxima on the first and second layer lines might profitably be analyzed from this perspective.

Conclusions

It has been suggested previously[11] that a side-chain length of six or more methylene units is necessary to provide sufficient intermolecular interactions to induce the silicon chain to assume a trans planar conformation. The diffraction pattern obtained for poly(*n*-butyl-*n*-hexylsilane) shows that the polymer adopts a 7/3 helical backbone conformation typical of PdnBS and PdnPS, although with some amount of intramolecular disordering of the side chains. Disorder introduced by the second, shorter substituent mitigates the intermolecular interactions which are therefore insufficient to force the backbone of poly(*n*-butyl-*n*-hexylsilane) into an all-trans conformation. On the other hand, an all-trans conformation is found for poly(*n*-pentyl-*n*-hexylsilane) and the other asymmetric polymers studied, suggesting that some disorder can be tolerated within the side chain packing and still lead to an all-trans backbone conformation.

For polysilanes having longer substituents, it has been found that a side-chain length of nine methylene units apparently allows the polymer backbone to adopt alternative conformations besides the 7/3 helix and all-trans. Polymers having nonyl or longer side chains adopt a TGTG′ backbone conformation and orthorhombic unit cells. Ambiguous results for the octyl-substituted polymer indicate that, under some circumstances, this polymer can also adopt a TGTG′ conformation. Spectroscopic data on PdnTDS are consistent with this backbone conformation. Further, the spectroscopic data indicate that the side chains are in a planar zigzag conformation (except perhaps very near the silicon backbone) and have a hexagonal packing mode.

Above their respective transition temperatures, all the polymer structures apparently transform to a columnar arrangement of cylindrical molecules on a hexagonal lattice as previously suggested.[20]

References and Notes

(1) Miller, R. D.; Hofer, D.; Rabolt, J. F.; Fickes, G. N. *J. Am. Chem. Soc.* **1985**, *107*, 2172.
(2) Miller, R. D.; Rabolt, J. F.; Sooriyakumaran, R.; Fleming, W.; Fickes, G. N.; Farmer, B. L.; Kuzmany, H. In *Inorganic and Organometallic Polymers*; Zeldin, M., Wynne, K. J., Allcock, H. R., Eds.; ACS Symposium Series 360; American Chemical Society: Washington, DC, 1988; p 43.
(3) Miller, R. D.; Michl, J. *Chem. Rev.* **1989**, *89*, 1390.
(4) Rabolt, J. F.; Hofer, D.; Miller, R. D.; Fickes, G. N. *Macromolecules* **1986**, *19*, 611.
(5) Lovinger, A. J.; Schilling, F. C.; Bovey, F. A.; Zeigler, J. M. *Macromolecules* **1986**, *19*, 2657.
(6) Schilling, F. C.; Bovey, F. A.; Lovinger, A. J.; Zeigler, J. M. *Macromolecules* **1986**, *19*, 2660.
(7) Schilling, F. C.; Lovinger, A. J.; Zeigler, J. M.; Davis, D. D.; Bovey, F. A. *Macromolecules* **1989**, *22*, 3055.
(8) Hallmark, V. M.; Sooriyakumaran, R.; Miller, R. D.; Rabolt, J. F. *J. Chem. Phys.* **1989**, *90*, 2486.
(9) Kuzmany, H.; Rabolt, J. F.; Farmer, B. L.; Miller, R. D. *J. Chem. Phys.* **1986**, *85*, 7413.
(10) Miller, R. D.; Farmer, B. L.; Fleming, W.; Sooriyakumaran, R.; Rabolt, J. F. *J. Am. Chem. Soc.* **1987**, *109*, 2509.
(11) Farmer, B. L.; Rabolt, J. F.; Miller, R. D. *Macromolecules* **1987**, *20*, 1167.
(12) Chapman, B. R.; Patnaik, S. S.; Farmer, B. L. *Polym. Prepr. (Am. Chem. Soc., Div. Polym. Chem.)* **1990**, *31* (2), 1265.
(13) Damewood, J. R., Jr. *Macromolecules* **1985**, *18*, 1793.
(14) Patnaik, S. S.; Farmer, B. L. *Polymer* **1992**, *33*, 4443.
(15) Schilling, F. C.; Bovey, F. A.; Lovinger, A. J.; Zeigler, J. M. *Bull. Am. Phys. Soc.* **1988**, *33* (3), 657.
(16) Michl, J.; Downing, J. W.; Katatsu, T.; Klingensmith, K. A.; Wallraff, G. M.; Miller, R. D. In *Inorganic and Organometallic Polymers*: Zeldin, M., Wynne, K. J., Allcock, H. R., Eds., ACS Symposium Series 360; American Chemical Society: Washington, DC, 1988; p 61.
(17) Farmer, B. L.; Miller, R. D.; Rabolt, J. F.; Fleming, W. W.; Fickes, G. N. *Bull. Am. Phys. Soc.* **1988**, *33*, 1657.
(18) Greso, A. J. M.S. Thesis, University of Virginia, Charlottesville, VA, 1989.
(19) Craubner, H. *Rev. Sci. Instrum.* **1986**, *57*, 2817.
(20) Weber, P.; Guillon, D.; Skoulios, A.; Miller, R. D. *J. Phys. Fr.* **1989**, *350*, 1793.
(21) Song, K.; Miller, R. D.; Wallraff, G. M.; Rabolt, J. F. *Macromolecules* **1991**, *24*, 4084.
(22) Lovinger, A. J.; Davis, D. D.; Schilling, F. C.; Bovey, F. A.; Padden, F. A.; Zeigler, J. M. *Macromolecules* **1991**, *24*, 132.
(23) Lovinger, A. J.; Davis, D. D.; Schilling, F. C.; Bovey, F. A.; Zeigler, J. M. *Polym. Commun.* **1989**, *30*, 356.
(24) SYBYL, Version 5.2, Tripos Associates, St. Louis, MO.
(25) Chapman, B. R.; Farmer, B. L. *Polym. Prepr. (Am. Chem. Soc., Div. Polym. Chem.)* **1990**, *31* (2), 1288.